Supplementary Appendix

CCND2 rearrangements are the most frequent genetic events in Cyclin D1-negative mantle cell lymphoma

Salaverria et al.

I. Supplemental Methods

FISH analysis

For the detection of the t(11;14)(q13;q32) a LSI (Locus Specific Identifier) *IGH/CCND1* double-color, double-fusion probe was used (Abbott-Vysis, Downers Grove, IL). *IGH@* breaks were studied using *IGH* Dual Color, Break apart rearrangement Probe (Abbott-Vysis). For break-apart FISH assays of *CCND2, CCND3*, *IGK@*, and *IGL@*, appropriate BAC/PAC clones flanking the respective genes were selected using bioinformatic resources available at the University of California at Santa Cruz (http://genome.ucsc.edu). BAC/PAC clones were obtained from Invitrogen (Karlsruhe, Germany) and differentially labeled with Spectrum Orange or Spectrum Green (supplementary Table S2). Bacterial culture, BAC/PAC DNA isolation and labeling, probe preparation, and FISH were performed as previously described.[1]

DNA extraction and array-comparative genomic hybridization (aCGH)

Genomic DNA was extracted from formalin-fixed, paraffin-embedded tissue (FFPE) blocks using the phenol-chloroform extraction method.[2] DNA quality control prior to hybridization was performed using standard protocols.[3] All extracted DNAs had at least a PCR control gene band of 200 bp (nine of the cases with a band of 200 bp, five cases with 400 bp, six cases with 300 bp and one cases with a 600 bp amplification band), and therefore all of them were suitable for hybridization. aCGH was performed in all samples hybridizing 1.5 µg of the test DNA and 1.5 µg of a sex-matched reference DNA on SurePrint G3 Human aCGH Microarray 1M (Agilent Technologies, Palo Alto, CA). The protocol Oligonucleotide Array-Based CGH for Genomic DNA Analysis (ULS

labeling for Blood, Cells, Tissues or FFPE) was used. aCGH hybridization was outsourced at qGenomics (www.qgenomics.com/). Protocol Version 3.1 was followed with slight modifications. Briefly, after digestion the DNA was fragmented (99ºC for 40 min) and labeled. After hybridization slides were washed and fluorescence was assessed using an Agilent microarray scanner G2565CA (Agilent Technologies). Raw data were generated from scanned images using Agilent Feature Extraction Software (v10.7). Log2ratios of background corrected values for tumor over normal DNA were calculated. Normalization was carried out on Agilent's CGH Analytics, integrated on the Genomic Workbench suite (v5.0). Detection of copy number alterations was performed using the Aberration Detection Method-2 (ADM-2) algorithm, implemented within the Agilent's genomics suite Genomic Workbench v5.0 and Nexus 6.0 Discovery Edition (Biodiscovery, El segundo, CA). The results were concordant with both algorithms. All alterations were confirmed by visual inspection of two different observers. Waves aCGH correction algorithm (WACA), based on GC content and fragment size adjusted was applied in several cases[4]. WACA efficiently removes the wave artifact, thereby greatly improving the accuracy of aCGH data analysis. Copy number variations/polymorphisms were identified and excluded from further analyses. Regions showing aberrant copy number changes were mapped according to the human reference sequence (NCBI36/hg18).

Cyclin D1, D2 and D3 and SOX11 gene expression assay

Total RNA was extracted from peripheral blood of three cases (ID17, ID36 and ID41) using the AllPrep DNA/RNA Mini Kit (Qiagen, Germantown, MA). The

potential residual DNA was removed using the TURBO DNA-free™ Kit form Ambion (Applied Biosystems, Santa Clara, US). Complementary DNA synthesis was carried out from 500 ng of total RNA and the product was amplified and quantified using TaqMan® Universal PCR Master Mix (Applied Biosystems) as previously described.[5] Cyclin D1, D2, D3 and E1 expression levels were evaluated using Gene Expression Assays-on-Demand Hs00765553_m1, Hs00153380_m1, Hs00236949_m1, and Hs01026536_m1, respectively (Applied Biosystems). Fluorescent probes TaqMan®MGB and primers were designed for evaluation of SOX11 expression using Primer Express® Version 2.0 (Applied Biosystems) probe: 5'-TTTTAACCACGGATAATTG-3', primer forward: 5'-CATGTAGACTAATGCAGCCATTGG-3', primer reverse: 5'-CACGGAGCACGTGTCAATTG-3'. We obtained an 87 bp amplicon for SOX11 that was suitable for FFPE material. The products were analyzed in a Step One Plus Real-Time PCR System (Applied Biosystems).

II. Supplemental Tables

Supplemental Table S1. Genetical, morphological and immunophenotypical characteristics of 41 cyclin D1-negative lymphomas.

Case	Transl.	LN Involvement	Growth pattern	Morphology	Mitosis	SOX11	CD5	p27	Ki67*	CD10	CD23
ID1	neg	LN (inguinal)	diffuse, monotonous	classical	1.6/hpf	pos	pos	neg	low	-	neg
ID2	neg	LN (multiple)	diffuse	classical	3.6/hpf	pos	pos	neg	-	-	neg
ID3	neg	LN	nodular	classical	2.4/hpf	pos	pos	neg	-	-	neg
ID4	neg	LN (multiple)	diffuse	classical	2.2/hpf	pos	pos	neg	-	-	w/pos
ID5	neg	LN	nodular	classical	-	pos	pos	neg	-	-	neg
ID6	neg	LN	nodular	classical	-	pos	pos	neg	-	-	neg
ID7	D2-K	LN (inguinal)	vaguely nodular, monotonous	classical	1.6/hpf	pos	pos	neg	-	neg	neg
ID8	neg	no	diffuse	classical	0.8/hpf	pos	pos	w/neg	low	neg	neg
ID9	neg	LN	diffuse	classical	0.2/hpf	pos	pos	w/neg	low	neg	neg
ID10	D2-K	LN	diffuse	classical	0.2/hpf	pos	pos	-	low	-	-
ID11	neg	LN (multiple)	diffuse	classical	1.2/hpf	pos	pos	w	low	neg	neg
ID12	neg	LN (inguinal)	vaguely nodular, diffuse	classical	0.1/hpf	pos	pos	neg	low	neg	neg
ID13	D2-K	LN (multiple)	nodular, diffuse, monotonous	classical	7/hpf	pos	pos	w	-	neg	neg
ID14	D2-H	LN (multiple)	diffuse	classical	-	pos	pos	neg	-	neg	neg
ID15	D2-K	LN (cervical)	diffuse	classical	-	pos	pos	neg	-	neg	neg
ID16	D2-?	LN (multiple)	diffuse	classical	-	pos	pos	neg	-	neg	neg
ID17	D2-K	LN (cervical)	diffuse	classical	-	pos (RT-PCR)	pos	-	-	neg	neg
ID18	D2-K	LN	vaguely nodular diffuse	classical	10/hpf	pos	pos	-	-	neg	-
ID23	neg	LN	diffuse	classical	10/hpf	pos w	w/neg	-	-	neg	-
ID24	D2-H	LN (cervical)	nodular	blastoid	4/hpf	pos	pos	-	high	-	neg
ID25	neg	LN (cervical)	vaguely	classical	1/hpf	pos	pos	w/neg	high	neg	neg

			nodular								
ID26	neg	LN (inguinal)	vaguely nodular	classical	8/hpf	pos	pos	pos	high	neg	neg
ID27	neg	LN (inguinal)	nodular, GC remnants, DLBCL-like areas	classical + pleomorphic component	1.4/hpf	pos†	pos	pos†	low	neg	neg
ID28	D2-K	LN (inguinal)	nodular	classical	2/hpf	pos	pos	w/neg	high	neg	neg
ID29	D2-break	LN (cervical)	Diffuse	classical	1.2/hpf	pos	pos	w	high	pos in a subset of cells	neg
ID30	neg	LN (axillary)	nodular	classical	6/hpf	pos	pos	-	high	neg	neg
ID31	D2-break	LN (periaortic)	nodular	classical	6/hpf	pos	pos	w/neg	high		neg
ID32	D2-K	LN (axillary)	Diffuse	classical	3/hpf	pos	pos	neg	high	neg	neg
ID33	neg	LN	nodular	classical	0.2/hpf	pos	pos	-	-	neg	neg
ID34	D2-?	LN	nodular	classical	0.6/hpf	pos	pos	neg	low	neg	neg
ID35	D2-L	LN (multiple)	Diffuse	classical		pos	pos	neg	-	-	-
ID36	D2-L	LN (mutiple)	-	-	-	pos (GEP, RT-PCR)	pos	-	-	-	neg
ID37	D2-L	LN (mutiple)	nodular	classical	0.4/hpf	pos	pos	-	low	-	-
ID38	neg	LN (mutiple)	nodular	classical	0.8/hpf	pos	pos	w	low	neg	neg
ID39	D2-L	LN (cervical)	Diffuse	classical	1/hpf	pos	pos	w	high	neg	neg
ID40	D2-K	LN (multiple)	Diffuse	classical	2.4/hpf	pos	pos	neg	low	neg	neg
ID42	D2-L	LN (inguinal)	mantle zone	classical	0.2/hpf	pos	pos w	w	low	neg	neg
ID43	D2-H	LN (mediastinal, subcranial)	Diffuse	classical	1.2/hpf	pos	pos	w	low	-	neg
ID44	D2-K	LN (inguinal)	nodular	classical	1.6/hpf	pos	pos	neg	low	neg	neg
ID45‡	neg	LN	nodular	classical	1.2/hpf	neg	pos	w	low	neg	neg
ID46	neg	-	Diffuse	classical	(high)	pos	pos	-	low	neg	-

D2-? indicates *CCND2* with unidentified partner discarding *IGH@, IGK@* or *IGL@*; D2-break, *CCND2* with unidentified partner; LN, lymph node; pos, positive; neg, negative; -, not available-not evaluable; w, weak; hpf: high power field; transl., translocation.

* ≥35% Ki67 was considered high proliferation.

†negative in the large cell component.

‡This case was excluded due to its SOX11-negativity.

Supplemental Table S2. Probes used for fluorescence *in situ* hybridization (FISH) analysis.

Probe name	**Company**	**Chromosomal band**	**Fluorescent dye**
LSI *IGH*@ BAP	Abbott, IL	**14q32**	Spectrum green/ orange
LSI *IGH/CCND1*	Abbott, IL	**14q32/11q13**	Spectrum green/ orange
Clone name	**Vector type**	**Genomic localization of insert***	**Fluorescent dye**
CCND2 BAP		**12p13**	
RP11-578L13	BAC	chr12:4,002,511-4,203,622	Spectrum orange
RP11-388F6	BAC	chr12:4,443,393-4,613,592	Spectrum green
CCND3 BAP		**6p21**	
RP5-973N23	PAC	41,802,166-41,918,671	Spectrum green
RP1-321B9	PAC	42,267,853-42,351,409	Spectrum orange
RP1-139D8	PAC	42,100,870-42,267,952	Spectrum orange
RP11-298J23	BAC	41,672,051-41,851,513	Spectrum green
IGK@ BAP		**2p11**	
RP11-316G9 (AC009958)	BAC	chr2:89,561,552-89,772,752	Spectrum orange
RP11-1021F11	BAC	chr2:88,767,510-88,939,350	Spectrum green
RP11-525L16 (AC104134)	BAC	chr2:88,570,647-88,680,773	Spectrum green
IGL@ BAP		**22q11**	
CTA-526G4	BAC	chr22:20,634,858-20,740,796	Spectrum green
clone 60B5 (AC000102)	BAC	chr22:21,835,020-21,838,494	Spectrum orange
CTA-865E9	BAC	chr22:27,735,801-27,843,216	Spectrum orange

BAC indicates bacteria artificial chromosome; BAP, break apart probe; LSI, Locus Specific Identifier; PAC, P1-derived artificial chromosome.
*NCBI Build 36.1/hg18.

Supplemental Table S3. Primers used for mutational analysis of Cyclin D genes.

Primer	Sequence	Amplicon Length (bp)
CCND1_F	CAGCAGAACATGGACCC	
CCND1_R	AGAATGAAGCTTTCCCTTCTG	222
CCND2_F	GTGCTCCTCAATAGCCTG	
CCND2_R	TCTCTTTCGGCCCAACTG	137
CCND3_F	CCTCTCAGACCAGCTCCA	
CCND3_R	TAGATGTGGTGTGGTTCCT	194

Bp indicates base pairs; F, forward; R, reverse.

Supplemental Table S4. Expression of cyclin D2, D3 and E in cyclin D1-negative MCL measured by IHC, RT-PCR and GEP.

		cyclin D2			cyclin D3			cyclin E1	
Case	**Transl.**	**IHC**	**qPCR**	**GEP**	**IHC**	**qPCR**	**GEP**	**IHC**	**qPCR**
ID1	neg	pos		pos					
ID2	neg			pos					
ID3	neg	na			pos		pos		
ID4	neg	na			pos		pos		
ID5	neg	na			pos		pos		
ID8	neg	neg			pos				
ID9	neg	na	neg		pos	pos			neg
ID11	neg	pos w	pos		neg				
ID12	neg		pos			neg			neg
ID23	neg							pos	
ID26	neg		neg			neg		pos w	neg
ID27	neg		neg			neg			neg
ID30	neg								
ID33	neg				pos				
ID38	neg								
ID46	neg		pos			neg			neg
ID7	D2-K	pos			neg				
ID13	D2-K	pos	pos			neg			
ID14	D2-H		pos			neg			
ID15	D2-K		pos			neg			
ID16	D2-?		pos			neg			
ID17	D2-K		pos			neg			
ID18	D2-K	pos							
ID28	D2-K		pos			neg			neg
ID29	D2-break		pos			neg			neg
ID31	D2-break		pos			neg			
ID34	D2-?	pos	pos			neg			neg
ID35	D2-L		pos			neg			
ID36	D2-L			pos					
ID39	D2-L		pos			neg			neg
ID40	D2-K		pos			neg			neg

GEP indicates gene expression proliling; IHC, immunohistochemistry; pos, positive; qPCR, quantitative PCR; Transl., translocation; w, weak

Supplemental Table S5. Complete FISH results of 40 Cyclin D1-negative MCL.

ID	Transl. Status	*CCND1 BAP*	*CCND2 BAP*	*CCND3 BAP*	*IGH@* BAP	*IGK@* BAP	*IGL@* BAP	*IGH-CCND1*	*IGH-CCND2*	*IGK-CCND2*	*IGL-CCND2*
ID1	neg	neg	neg	neg				neg			
ID2	neg	neg	neg	neg				neg			
ID3	neg	neg	neg	neg	neg*			neg			
ID4	neg	neg	neg	neg				neg			
ID5	neg	neg	neg	neg				neg			
ID6	neg	neg	neg	neg	neg*	neg*	neg*	neg			
ID7	D2-K		pos*		neg*	pos*	neg*	neg		pos*	
ID8	neg		neg	neg				neg			
ID9	neg		neg	neg				neg			
ID10	D2-K		pos	neg	neg*	pos*	neg*	neg			
ID11	neg		neg	neg				neg			
ID12	neg		neg	neg				neg			
ID13	D2-K	neg	pos	neg	neg	pos		neg		pos	
ID14	D2-H	neg	pos		pos				pos		
ID15	D2-K		pos			pos		neg		pos	
ID16	D2-?	neg	pos		neg	neg		neg			
ID17	D2-K	neg	pos		neg	pos		neg		pos	
ID18	D2-K	neg	pos	neg	neg	pos	neg			pos	
ID23	neg	neg	neg	neg	pos	neg	neg				
ID24	D2-H		pos	neg	pos	neg	neg	neg	pos		
ID25	neg		neg	neg				neg			
ID26	neg		neg	neg				neg			
ID27	neg		neg	neg				neg			
ID28	D2-K		pos		neg	pos	neg	neg		pos	
ID29	D2 break		pos		neg.	neg	neg	neg			
ID30	neg	neg	neg	na				neg			
ID31	D2-break		pos	neg	neg	neg	neg	neg			
ID32	D2-K		pos			pos		neg			
ID33	neg		neg	neg				neg			
ID34	D2-?		pos	neg				neg			
ID35	D2-L	neg	pos		neg	neg	pos				pos
ID36	D2-L		pos		neg	neg	pos	neg			pos
ID37	D2-L	neg	pos		neg	neg	pos	neg			
ID38	neg		neg	neg							
ID39	D2-L		pos		neg	neg	pos	neg			pos
ID40	D2-K		pos		neg	pos	neg	neg		pos	
ID42	D2-L		pos					neg	neg	neg	pos
ID43	D2-H		pos					neg	pos	neg	
ID44	D2-K		pos					neg	neg	pos	
ID46	neg		neg	neg				neg			

BAP indicates break apart probe; D2-?, *CCND2* break with unidentified partner discarding *IGH@, IGK@, IGL@*; D2-break, *CCND2* break with unidentified partner; neg, negative, pos: positive; transl, translocation.
*New FISH data of previously published cases.

Supplemental Table S6. Molecular data of 40 Cyclin D1-negative MCL.

Case	Transl. Status	CN array	No. CNA	9p21/ *CDKN2A*	11q23/ *ATM*	17p13/ *TP53*	*TP53* status	*CCND1* mut	*CCND2* mut	*CCND3* mut
ID1	neg	Affymetrix 500K /CGH	7	del	CNN-LOH	wt				
ID2	neg	Affymetrix 500K /CGH	2	del	wt	wt		wt	wt	wt
ID3	neg	Affymetrix 500K /CGH	27	del	del	wt		wt	wt	wt
ID4	neg	Affymetrix 500K /CGH	9	homo del	del	wt		wt	wt	wt
ID5	neg	Affymetrix 500K /CGH	10	wt	del	wt		wt	wt	wt
ID6	neg	Affymetrix 500K /CGH	7	wt	del	wt		wt	wt	wt
ID7	D2-K	na	na	na	na	na				
ID8	neg	Agilent 1M*	3	wt	del	wt		wt	wt	wt
ID9	neg	Agilent 1M*	7	wt	wt	wt		wt	wt	wt
ID10	D2-K	na	na	na	na	na				
ID11	neg	na	na	na	na	na				
ID12	neg	Agilent 1M*	4	wt	del	wt		wt	wt	wt
ID13	D2-K	Agilent 1M*	8	homo del	wt	wt				
ID14	D2 -H	Agilent 1M*	12	wt	del	del	na			
ID15	D2-K	Agilent 1M*	17	del	wt	wt				
ID16	D2-?	Agilent 1M*	10	del	wt	wt				
ID17	D2-K	Agilent 1M*	2	wt	wt	wt				
ID18	D2-K	Agilent 1M*	8	del	wt	del	exon 8 c.818G>A p.R273H			
ID23	neg	Agilent 1M*	16	homo del	wt	wt				
ID24	D2-H	na	na	na	na	na				
ID25	neg	Agilent 1M	15	wt	wt	wt		wt	wt	wt
ID26	neg	Agilent 1M	18	homo del	wt	wt		wt	wt	wt
ID27	neg	Agilent 1M	7	wt	del	wt		wt	wt	wt
ID28	D2-K	Agilent 1M	9	wt	wt	wt				
ID29	D2-neg	Agilent 1M	10	wt	gain	wt				
ID30	neg	Agilent 1M	30	homo del	del	wt			wt	wt
ID31	D2-neg	Agilent 1M	30	del	wt	wt				
ID32	D2-K	Agilent 1M	6	wt	del	del	na			

ID33	neg	na	na	na	na	na	
ID34	D2-?	Agilent 1M	3	wt	wt	del	wt
ID35	D2-L	Agilent 1M	14	wt	wt	Small homo del	homo del (promoter-exon 1)
ID36	D2-L	Agilent 1M	7	homo del	wt	wt	
ID37	D2-L	Agilent 1M	6	wt	wt	wt	
ID38	neg	Agilent 1M	14	wt	wt	del	wt exon 7 and 10. Others na
ID39	D2-L	Agilent 1M	13	homo del	wt	wt	
ID40	D2-K	Agilent 1M	6	del	wt	del	exon 7 c.723delC p.S241fs*5
ID42	D2-L	Agilent 1M	5	wt	del	wt	
ID43	D2-H	na	na	na	na	na	
ID44	D2-K	na	na	na	na	na	
ID46	neg	na	na	na	na	na	

CN indicates copy number; CNN-LOH, copy number neutral-loss of heterozygosity; D2-?, *CCND2* break with unidentified partner discarding *IGH@, IGK@ and IGL@* genes; D2-break, *CCND2* break with unidentified partner; del, deletion; homo del, homozygous deletion; mut, mutation; na, not available; neg, negative; transl., translocation; wt, wild type (no deletion/no CNN-LOH or no mutation).

*New copy number data of previously published cases.

Supplemental Table S7. Copy number alterations of 32 Cyclin D1-negative MCL.

Chromosome Region	Event	Length (bp)	Cytoband
ID1			
chr1:51,993,505-120,217,562	loss	68224057	p32.3-p12
chr1:120,233,802-145,938,656	loss	25704854	p12-q21.1
chr1:148,815,736-150,433,200	loss	1617464	q21.2-q21.3
chr1:152,683,489-164,496,493	loss	11813004	q21.3-q24.1
chr1:178,210,240-182,622,710	loss	4412470	q25.2-q25.3
chr8:180,568-38,755,604	loss	38575036	p23.3-p11.23
chr9:30,910-35,589,966	loss	35559056	p24.3-p13.3
ID2			
chr9:0-140,273,252	loss	140273252	p24.3-q34.3
chr13:16,000,001-114,142,980	loss	98142979	q11 - q34
ID3			
chr1:92833128-108105451	loss	15272323	p22.1-p13.3
chr3:122157217-143336624	gain	21179407	q13.33-q23
chr3:143391891-155982031	loss	12590140	q23-q25.2
chr3:155991502-199322068	gain	43330566	q25.2-q29
chr4:19099-1869140	loss	1850041	p16.3
chr6:99676430-107549664	loss	7873234	q16.2-q21
chr6:114619068-124346399	loss	9727331	q22.1-q22.31
chr8:180568-4155262	loss	3974694	p23.3-p23.2
chr8:4164397-12517929	loss	8353532	p23.2-p23.1
chr8:12632654-39663381	loss	27030727	p23.1-p11.22
chr8:39928509-41380701	loss	1452192	p11.21
chr8:41481725-47059642	loss	5577917	p11.21-q11.1
chr8:47064078-47847875	gain	783797	q11.1
chr8:47851472-49520992	loss	1669520	q11.1-q11.21
chr8:49687681-49820725	loss	133044	q11.21
chr8:49838874-77957795	gain	28118921	q11.21-q21.11
chr8:78051789-85298711	gain	7246922	q21.11-q21.2
chr8:85305933-87855113	loss	2549180	q21.2-q21.3
chr8:87858448-146264218	gain	58405770	q21.3-q24.3
chr9:3697057-3763822	loss	66765	p24.2
chr9:4272942-97248353	loss	92975411	p24.2-q22.32
chr9:98238862-109511513	loss	11272651	q22.33-q31.2
chr9:110631769-110750958	loss	119189	q31.3
chr11:95814925-116253431	loss	20438506	q21.3-q23.3
chr13:16,000,001-114,142,980	loss	98142979	q11 - q34
chr22:15405346-17348025	gain	1942679	q11.1-q22.1
chr22:21967766-49519949	loss	27552183	q11.23-q13.33
ID4			
chr3:107,270,190-199322,068	gain	92051878	q13.11-q29
chr4:53,377,961-96,814,371	loss	43436410	q12-q22.3
chr9:21,757,404-22,231,938	homo del	474534	p21.3
chr11:84,251,805-114,988,378	loss	30736573	q14.1-q23.2
chr13:85,305,104-114,092,980	loss	28787876	q31.1-q34
chr14:19,865,555-45,099,437	loss	25233882	q11.2-q21.3
chr15:53,360,818-86,623,678	gain	33262860	q21.3-q25.3
chr15:86,625,685-100,210,760	loss	13585075	q25.3-q26.3
chr17:51,265,658-78,605,474	gain	27339816	q22-q25.3
ID5			
chr1:73,687,779-89,945,089	loss	16257310	p31.1-p22.2
chr1:92,498,763-106,592,214	loss	14093451	p22.1-p21.1

chr1:107,364,675-112,046,454	loss	4681779	p13.3-p13.2
chr1:149,495,781-178,520,303	loss	29024522	q21.2-q25.2
chr3:41,866-47,887,707	loss	47845841	p26.3-p21.31
chr3:70,451,282-75,779,859	loss	5328577	p14.1-p12.3
chr3:75,879,418-79,985,503	loss	4106085	p12.3
chr11:99,008,430-116,960,909	loss	17952479	q22.1-q23.3
chr12:36,144,018-43,299,888	loss	7155870	q11-q12
chr20:17,408-28,143,658	loss	28126250	p13-q11.1
ID6			
chr3:135,289,282-199,322,068	gain	64032786	q22.1-q29
chr4:112,976,431-191,306,043	gain	78329612	q25-q35.2
chr11:93,480,063-113,841,400	loss	20361337	q21-q23.2
chr13:49,167,094-50,232,139	loss	1065045	q14.3
chr13:85,422,217-108,460,875	gain	23038658	q31.1-q33.3
chr13:108,469,059-114,092,980	loss	5623921	q33.3-q34
chr18:61,496,779-76,115,554	gain	14618775	q22.1-q23
ID8			
chr1:68,813,528-118,010,981	loss	49197454	p31.2 - p12
chr11:102,431,516-116,476,458	loss	14044943	q22.3 - q23.3
chr12:10,972,665-14,943,904	loss	3971240	p13.2 - p12.3
ID9			
chr1:73,978,016-121,233,935	loss	47255920	p31.1 - p11.1
chr1:152,015,948-170,010,522	loss	17994575	q21.3 - q24.3
chr1:174,539,409-176,471,597	loss	1932189	q25.2
chr12:12,774,282-15,124,635	loss	2350354	p13.1 - p12.3
chr13:17,920,058-114,142,980	loss	96222923	q11 - q34
chr18:86,595-14,980,964	loss	14894370	p11.32 - p11.21
chr18:49,103,401-76,117,153	gain	27013753	q21.2 - q23
ID12			
chr1:89,671,879-119,855,488	loss	30183609	p22.2 - p12
chr7:136,173-80,019,908	gain	79883735	p22.3 - q21.11
chr7:135,249,024-158,767,981	gain	23518957	q33 - q36.3
chr11:79,476,627-114,249,985	loss	34773358	q14.1 - q23.2
ID13			
chr1:74,410,664-79,209,473	loss	4798810	p31.1
chr3:119,704,364-165,177,987	gain	45473624	q13.32 - q26.1
chr3:165,223,275-199,501,827	high gain	34278553	q26.1 - q29
chr3:29,751,203-34,407,204	gain	4656002	p24.1 - p22.3
chr6:91,289,881-170,899,992	loss	79610112	q15 - q27
chr9:21,073,742-22,513,201	homo del	1439460	p21.3
chr13:38,594,462-57,403,763	loss	18809302	q13.3 - q21.1
chr13:82,780,288-88,825,160	loss	6044873	q31.1 - q31.3
ID14			
chr1:233,483,703-247,249,719	loss	13766017	q42.3 - q44
chr3:146,954,760-199,274,862	gain	52320103	q24 - q29
chr3:68,259,584-82,217,903	loss	13958320	p14.1 - p12.2
chr7:180,684-43,725,580	high gain	43544897	p22.3 - p13
chr7:43,725,580-158,640,740	gain	114915161	p13 - q36.3
chr8:71,679,759-141,964,056	gain	70284298	q13.3 - q24.3
chr11:78,806,216-117,595,915	loss	38789700	q14.1 - q23.3
chr15:76,070,289-100,293,722	loss	24223434	q24.3 - q26.3
chr17:89,619-3,405,506	loss	3315888	p13.3
chr18:12,141,770-75,884,693	gain	63742924	p11.21 - q23
chr18:86,595-12,123,324	loss	12036730	p11.32 - p11.21

chrX:176,239-154,737,515	gain	154561277	p22.33 - q28
ID15			
chr3:103,031,571-199,159,185	gain	96127615	q12.3 - q29
chr4:82,277,484-87,121,650	loss	4844167	q21.21 - q21.3
chr4:98,786,025-116,258,391	gain	17472367	q22.3 - q26
chr4:117,753,722-120,119,804	loss	2366083	q26
chr6:337,275-25,928,580	gain	25591306	p25.3 - p22.2
chr6:85,014,643-170,899,992	loss	85885350	q14.3 - q27
chr8:116,154,526-138,120,712	gain	21966187	q23.3 - q24.23
chr8:138,182,510-146,084,009	high gain	7901500	q24.23 - q24.3
chr9:21,779,871-23,781,282	loss	2001412	p21.3
chr9:134,894,698-140,273,252	gain	5378555	q34.13 - q34.3
chr11:59,501,681-71,585,570	gain	12083890	q12.1 - q13.4
chr12:49,085,265-132,198,966	gain	83113702	q13.13 - q24.33
chr13:37,528,238-74,926,621	loss	37398384	q13.3 - q22.2
chr13:100,433,003-114,142,980	loss	13709978	q32.3 - q34
chr15:49,779,890-100,338,915	gain	50559026	q21.2 - q26.3
chr19:72,596-63,739,055	gain	63666460	p13.3 - q13.43
chr22:15,489,707-49,634,900	gain	34145194	q11.1 - q13.33
ID16			
chr2:230,745,327-231,313,360	loss	568034	q37.1
chr3:62,244,056-84,397,240	loss	22153185	p14.2 - p12.1
chr3:128,142,008-199,067,780	gain	70925773	q21.3 - q29
chr8:114,816,427-146,054,649	gain	31238223	q23.3 - q24.3
chr9:20,094,175-33,737,685	loss	13643511	p21.3 - p13.3
chr10:122,294,405-129,001,459	loss	6707055	q26.12 - q26.2
chr10:129,937,783-132,104,961	loss	2167179	q26.2 - q26.3
chr13:99,532,408-114,142,980	loss	14610573	q32.3 - q34
chr15:32,530,368-100,131,521	gain	67601154	q14 - q26.3
chr22:22,900,000-30,774,569	loss	7874570	q11.23 - q12.3
ID17			
chr3:226,965-199,274,862	gain	199047898	p26.3 - q29
chr21:14,152,725-46,890,916	gain	32738192	q11.2 - q22.3
ID18			
chr1:234,554,474-237,835,442	loss	3280969	q42.3 - q43
chr2:134,331,342-146,899,054	loss	12567713	q21.2 - q22.3
chr3:0-199,501,827	gain	199501828	p26.3 - q29
chr6:194,425-26,682,076	gain	26487652	p25.3 - p22.1
chr9:20,608,317-32,351,699	loss	11743383	p21.3 - p21.1
chr15:38,792,251-48,275,906	loss	9483656	q15.1 - q21.2
chr17:0-22,135,792	loss	22135793	p13.3 - p11.1
chr19:0-63,811,651	loss	63811652	p13.3 - q13.43
ID23			
chr2:37,857,137-39,765,052	loss	1907916	p22.2 - p22.1
chr4:87,021,902-191,055,460	gain	104033559	q21.23 - q35.2
chr6:100,519,055-106,968,270	loss	6449216	q16.3 - q21
chr6:108,842,051-109,945,426	loss	1103376	q21
chr6:133,291,911-145,951,050	loss	12659140	q23.2 - q24.3
chr9:5,787,087-6,815,923	loss	1028837	p24.1
chr9:21,785,243-22,035,541	homo del	250299	p21.3
chr9:22,035,541-27,748,165	loss	5712625	p21.3 - p21.2
chr9:34,850,892-38,751,707	loss	3900816	p13.3 - p13.1
chr10:87,680,312-88,090,573	loss	410262	q23.1 - q23.2
chr10:89,654,536-90,171,763	loss	517228	q23.31

chr13:37,055,769-61,845,186	loss	24789418	q13.3 - q21.31
chr15:22,657,953-46,785,947	loss	24127995	q11.2 - q21.1
chr16:74,038-31,910,354	gain	31836317	p13.3 - p11.2
chr18:16,798,083-76,117,153	gain	59319071	q11.1 - q23
chr21:12,860,650-46,944,323	gain	34083674	q11.1 - q22.3
ID25			
chr3:0-27,689,673	loss	27689674	p26.3 - p24.1
chr3:27,703,100-31,603,069	gain	3899970	p24.1 - p23
chr3:31,606,294-35,729,732	high gain	4123439	p23 - p22.3
chr3:35,733,527-51,846,193	gain	16112667	p22.3 - p21.1
chr3:75,958,756-84,186,801	gain	8228046	p12.3 - p12.1
chr3:124,837,607-199,501,827	gain	74664221	q21.1 - q29
chr5:49,580,889-72,351,948	gain	22771060	q11.1 - q13.2
chr5:72,396,367-118,201,085	loss	45804719	q13.2 - q23.1
chr8:0-75,198,612	loss	75198613	p23.3 - q21.11
chr10:123,084,428-135,374,737	loss	12290310	q26.12 - q26.3
chr13:45,086,087-114,142,980	loss	69056894	q14.12 - q34
chr14:17,546,581-106,368,585	loss	88822005	q11.1 - q32.33
chr18:50,362,627-76,080,308	gain	25717682	q21.2 - q23
chr19:72,596-24,174,380	loss	24101785	p13.3 - p12
chr22:15,150,516-49,691,432	loss	34540917	q11.1 - q13.33
ID26			
chr1:143,432,108-247,249,719	gain	103817612	q21.1 - q44
chr4:142,330,704-191,273,063	loss	48942360	q31.21 - q35.2
chr6:0-33,088,385	gain	33088386	p25.3 - p21.32
chr6:105,229,233-170,899,992	loss	65670760	q21 - q27
chr7:0-30,339,319	gain	30339320	p22.3 - p15.1
chr9:0-21,959,807	loss	21959808	p24.3 - p21.3
chr9:21,959,807-22,027,830	homo del	68024	p21.3
chr9:22,027,830-30,700,306	loss	8672477	p21.3 - p21.1
chr10:27,967,434-38,665,781	loss	10698348	p12.1 - p11.21
chr11:57,402,170-63,452,380	loss	6050211	q12.1 - q13.1
chr12:17,029,319-132,349,534	gain	115320216	p12.3 - q24.33
chr13:21,363,962-57,006,562	loss	35642601	q12.11 - q21.1
chr17:49,101,131-78,774,742	gain	29673612	q22 - q25.3
chr18:0-56,546,645	gain	56546646	p11.32 - q21.32
chr18:61,526,155-76,117,153	loss	14590999	q22.1 - q23
chr21:14,152,725-46,944,323	gain	32791599	q11.2 - q22.3
chrX:0-10,750,556	loss	10750557	p22.33 - p22.2
chrX:78,161,130-154,913,754	gain	76752625	q21.1 - q28
ID27			
chr1:80,619,100-85,090,543	loss	4471444	p31.1 - p22.3
chr1:99,871,298-109,071,469	loss	9200172	p21.2 - p13.3
chr2:167,393,190-170,790,488	loss	3397299	q24.3 - q31.1
chr8:57,195,231-69,304,008	loss	12108778	q12.1 - q13.2
chr8:115,177,456-146,274,826	gain	31097371	q23.3 - q24.3
chr11:75,473,101-117,610,184	loss	42137084	q13.5 - q23.3
chr18:48,394,049-76,117,153	gain	27723105	q21.2 - q23
ID28			
chr1:59,457,106-110,871,182	loss	51414077	p32.1 - p13.3
chr3:47,829,355-68,228,276	gain	20398922	p21.31 - p14.1
chr13:94,004,590-114,142,980	loss	20138391	q32.1 - q34
chr15:38,765,310-42,992,281	loss	4226972	q15.1 - q21.1
chr15:43,020,462-100,338,915	gain	57318454	q21.1 - q26.3

chr18:47,954,940-76,117,153	high gain	28162214	q21.2 - q23
chr19:0-7,912,935	loss	7912936	p13.3 - p13.2
chrY:2,563,305-18,074,587	gain	15511283	p11.31 - q11.221
chrY:19,257,651-27,210,470	loss	7952820	q11.22 - q12
ID29			
chr1:5,731,947-9,577,458	loss	3845512	p36.31 - p36.22
chr3:148,977,817-199,501,827	gain	50524011	q24 - q29
chr6:92,147,279-127,338,511	loss	35191233	q16.1 - q22.33
chr11:58,583,917-77,398,073	gain	18814157	q12.1 - q14.1
chr11:98,046,539-134,452,384	gain	36405846	q22.1 - q25
chr13:51,221,123-68,670,806	loss	17449684	q14.3 - q21.33
chr13:68,682,477-100,508,153	gain	31825677	q21.33 - q33.1
chr13:100,508,171-114,127,451	loss	13619281	q33.1 - q34
chr19:0-19,818,636	gain	19818637	p13.3 - p12
chr19:40,062,439-55,007,746	gain	14945308	q13.11 - q13.33
ID30			
chr1:33,485,277-34,856,481	loss	1371205	p35.1 - p34.3
chr1:37,950,366-40,203,347	loss	2252982	p34.3 - p34.2
chr1:40,762,476-42,278,709	loss	1516234	p34.2
chr1:43,708,473-46,315,579	loss	2607107	p34.2 - p34.1
chr1:5,714,458-6,789,871	loss	1075414	p36.31
chr1:51,495,144-53,559,489	loss	2064346	p32.3
chr1:66,938,205-74,368,743	loss	7430539	p31.3 - p31.1
chr1:77,599,391-85,721,054	loss	8121664	p31.1 - p22.3
chr1:86,226,477-86,936,769	loss	710293	p22.3
chr1:92,007,479-121,052,453	loss	29044975	p22.1 - p11.2
chr1:143,597,231-159,736,731	loss	16139501	q21.1 - q23.3
chr1:161,239,479-175,980,553	loss	14741075	q23.3 - q25.2
chr1:182,837,574-185,658,629	loss	2821056	q25.3 - q31.1
chr1:235,994,921-237,567,794	loss	1572874	q43
chr2:33,314,713-44,243,800	loss	10929088	p22.3 - p21
chr2:47,539,929-148,147,686	loss	100607758	p21 - q22.3
chr3:31,760-12,545,019	loss	12513260	p26.3 - p25.1
chr6:105,758,502-170,899,992	loss	65141491	q21 - q27
chr7:105,253,295-129,532,052	loss	24278758	q22.2 - q32.2
chr9:21,917,964-32,189,162	homo del	10271199	p21.3 - p21.1
chr9:3,538,540-21,878,969	loss	18340430	p24.2 - p21.3
chr9:32,189,162-39,146,954	loss	6957793	p21.1 - p13.1
chr10:58,968,027-60,093,859	loss	1125833	q21.1
chr11:106,731,698-114,299,361	loss	7567664	q22.3 - q23.2
chr11:123,309,407-126,282,577	loss	2973171	q24.1 - q24.2
chr11:78,627,253-79,720,573	loss	1093321	q14.1
chr11:80,163,644-82,876,083	loss	2712440	q14.1
chr11:95,266,025-95,876,733	loss	610709	q21
chr12:9,867,619-16,404,236	loss	6536618	p13.31 - p12.3
chr13:18,194,544-114,142,980	loss	95948437	q11 - q34
ID31			
chr2:6,819-576,621	loss	569802	p25.3
chr2:795,628-65,054,286	gain	64258658	p25.3 - p14
chr2:65,087,982-69,651,854	loss	4563872	p14
chr3:68,749-10,115,254	loss	10046505	p26.3 - p25.3
chr3:10,307,233-17,419,855	gain	7112622	p25.3 - p24.3
chr3:17,421,189-58,556,421	loss	66373407	p24.3 - p14.2
chr3:58,556,422-59,636,927	gain	1080505	p14.2

chr3:59,636,928-83,794,596	loss	24157668	p14.2-p12.1
chr4:95,351,472-97,821,365	loss	2469893	q22.2 - q22.3
chr4:97,908,661-149,148,031	gain	51239370	q22.3 - q31.23
chr4:172,766,175-183,888,171	loss	11121996	q34.1 - q35.1
chr4:183,897,426-190,286,409	gain	6388983	q35.1 - q35.2
chr6:44,345,592-137,291,465	loss	92945873	p21.1 - q23.3
chr6:137,291,466-138,816,901	gain	1525435	q23.3
chr6:138,816,902-156,192,098	loss	17375196	q23.3-q25.3
chr6:156,192,099-158,435,910	gain	2243811	q25.3
chr6:158,435,911-170,701,979	loss	12266068	q25.3-q27
chr7:136173-52685750	gain	52549577	p22.3 - p12.1
chr9:6591209-44199601	loss	37608392	p24.1 - p11.2
chr9:85112843-90024559	loss	4911716	q21.32 - q22.1
chr10:126161-2749287	loss	2623126	p15.3
chr10:2766712-38476892	gain	35710180	p15.3 - p11.21
chr10:42882274-60893302	loss	18011028	q11.21 - q21.1
chr10:107640100-112960080	loss	5319980	q25.1 - q25.2
chr10:126429421-135285845	loss	8856424	q26.13 - q26.3
chr13:18361437-114105156	loss	95743719	q11 - q34
chr13:49162155-50902584	homo del	1740429	q14.3
chr16:58424523-88827254	gain	30402731	q21-qter
chr18:37290171-76116226	gain	38826055	q12.3 - q23
chr19:3329679-5377839	loss	2048160	p13.3
ID32			
chr1:2,891,601-7,282,760	loss	4391160	p36.32 - p36.23
chr3:64,657,420-82,604,850	loss	17947431	p14.1 - p12.2
chr3:127,905,418-199,419,815	gain	71514398	q21.3 - q29
chr11:88,279,111-115,999,479	loss	27720369	q14.3 - q23.3
chr17:0-15,862,491	loss	15862492	p13.3 - p12
chr18:46,495,596-76,117,153	gain	29621558	q21.2 - q23
ID34			
chr3:137,317,818-199,430,186	gain	62112369	q22.2 - q29
chr13:18,049,914-114,013,125	loss	95963212	q11 - q34
chr17:0-37,460,571	loss	37460572	p13.3 - q21.2
ID35			
chr3:120,717,330-199,501,827	gain	78784498	q13.33 - q29
chr6:0-100,323,545	gain	100323546	p25.3 - q16.3
chr6:100,327,723-170,899,992	loss	70572270	q16.3 - q27
chr9:70,154,146-75,911,108	loss	5756963	q13 - q21.13
chr10:0-12,378,074	loss	12378075	p15.3 - p13
chr13:44,766,611-67,847,797	loss	23081187	q14.12 - q21.33
chr13:90,509,280-114,142,980	loss	23633701	q31.3 - q34
chr15:46,415,909-100,338,915	gain	53923007	q21.1 - q26.3
chr16:45,058,242-63,073,190	loss	18014949	q11.2 - q21
chr17:4,925,707-7,447,513	loss	2521807	p13.2 - p13.1
chr17:7,447,513-7,515,707	homo del	68195	p13.1
chr17:7,515,707-22,200,000	loss	14684294	p13.1 - q11.1
chr17:35,614,061-37,604,226	loss	1990166	q21.2
chr18:22,373,429-76,117,153	gain	53743725	q11.2 - q23
ID36			
chr8:0-39,450,836	loss	39450837	p23.3 - p11.23
chr8:129,357,472-140,613,631	gain	11256160	q24.21 - q24.3
chr9:134,764,651-140,273,252	loss	5508602	q34.13 - q34.3
chr9:21,203,515-22,082,128	homo del	878614	p21.3

chr10:0-1,457,845	loss	1457846	p15.3
chr11:0-4,331,622	loss	4331623	p15.5 - p15.4
chr19:0-19,818,636	loss	19818637	p13.3 - p12
ID37			
chr1:0-55,413,191	loss	55413192	p36.33 - p32.3
chr5:205,754-44,031,380	gain	43825627	p15.33 - p12
chr7:6,685,316-53,482,527	gain	46797212	p22.1 - p12.1
chr13:95,209,783-114,142,980	loss	18933198	q32.1 - q34
chr14:59,600,968-93,854,901	loss	34253934	q23.1 - q32.13
chr19:0-63,811,651	loss	63811652	p13.3 - q13.43
ID38			
chr4:20,287,021-35,043,814	loss	14756793	p15.31 - p15.1
chr7:0-158,821,317	gain	158821318	pter-qter
chr8:0-146,264,902	gain	146264903	pter-qter
chr12:33654-33968005	gain	33934351	p13.33 - p11.1
chr13:43415370-114115907	loss	70700537	q14.11 - q34
chr16:37,360-2,068,695	loss	2031335	p13.3
chr16:2,191,556-4,325,681	gain	2134125	p13.3
chr16:5,731,466-5,771,994	loss	40528	p13.3
chr16:5,791,237-664,4817	gain	853580	p13.3 - p13.2
chr16:6,660,422-8,066,557	loss	1406135	p13.2
chr16:8,090,486-16,169,516	gain	8079030	p13.2 - p13.11
chr17:48,658-38,550,415	loss	38501757	p13.3-q21.31
chr17:36,381,308-78,653,589	gain	42272281	q21.2-qter
chr18:32,868,064-76,116,226	gain	43248162	q12.2 - q23
ID39			
chr3:0-26,997,021	loss	26997022	p26.3 - p24.1
chr3:27,004,907-45,264,320	high gain	18259414	p24.1 - p21.31
chr3:59,801,661-76,296,630	loss	16494970	p14.2 - p12.3
chr3:88,780,987-90,391,757	loss	1610771	p11.2 - p11.1
chr3:101,938,062-103,852,930	gain	1914869	q12.2 - q12.3
chr6:105,736,247-144,652,990	loss	38916744	q21 - q24.2
chr9:1,471,834-2,400,093	loss	928260	p24.3 - p24.2
chr9:14,666,611-17,621,523	loss	2954913	p22.3 - p22.2
chr9:21,203,515-22,408,114	homo del	1204600	p21.3
chr9:22,408,114-24,561,146	loss	2153033	p21.3
chr9:33,977,890-37,590,163	loss	3612274	p13.3 - p13.2
chr9:88,325,406-89,792,312	loss	1466907	q21.33 - q22.1
chr13:97,113,864-114,142,980	loss	17029117	q32.2 - q34
ID40			
chr3:122,031,782-199,501,827	gain	77470046	q13.33 - q29
chr8:122,476,421-146,274,826	gain	23798406	q24.12 - q24.3
chr9:0-140,273,252	loss	140273253	p24.3 - q34.3
chr13:28,720,872-114,142,980	loss	85422109	q12.3 - q34
chr15:18,378,345-38,012,353	loss	19634009	q11.1 - q15.1
chr17:0-22,135,792	loss	22135793	p13.3 - p11.1
ID42			
chr11:93,107,599-113,904,326	loss	20796728	q21 - q23.2
chr13:18,309,625-46,228,556	loss (subclonal)	27918932	q11 - q14.2
chr13:46,589,758-114,142,980	loss	67553223	q14.2 - q34
chr14:18,635,679-106,368,585	loss (subclonal)	87732907	q11.1 - q32.33
chr22:14,867,857-49,691,432	loss (subclonal)	34823576	q11.1 - q13.33

Bp indicates base pairs; del: deletion; homo del, homozygous deletion.

Supplemental Table S8. Chromosomal regions (>5Mb) characteristic of cyclin D1 positive- and -negative MCL.

Cyclin D1-negative *vs.* Cyclin D1-positive MCL		
Region	**Size (Mb)**	**Chr. Band**
Frequent Deletions		
chr10:126429421-132104961	5,68	10q26.13-q26.3
chr13:100433003-114142980	13,71	13q32.3-q34
chr19:4368845-17399478	13,03	19p13.3-p13.11
Frequent Gains		
chr3:27703100-36473790	8,77	3p24.1-p22.3
chr4:110232094-125093640	14,86	4q25-q28.1
chr4:143344366-149148031	5,80	4q31.21-q31.23
chr6:5869499-26682076	20,81	6p25.1-p22.1
chr18:46495596-76117153	29,62	18q21.2-q23
CyclinD1-positive *vs.* Cyclin D1-negative		
Region	**Size (Mb)**	**Chr. Band**
Frequent Deletions		
chr1:55413191-103469102	48,06	1p32.3-p21.1
chr9:78852665-98238862	19,39	9q21.13-q22.33

Chr, indicates chromosome; Mb, megabases.

III. Supplemental Figures

Supplemental Figure S1. Cyclin D1, D2, D3 and E1 expression analyzed by qPCR in lymphoid neoplasms. (A) Box plot representing cyclin D2 expression and **(B)** bar plot with cyclin D1, D2, D3 and E1 expression analyzed in cyclin D1-negative MCL with presence/absence of *CCND2* rearrangements, in MCL cyclin D1-positive and in other lymphoid neoplasms non-MCL.

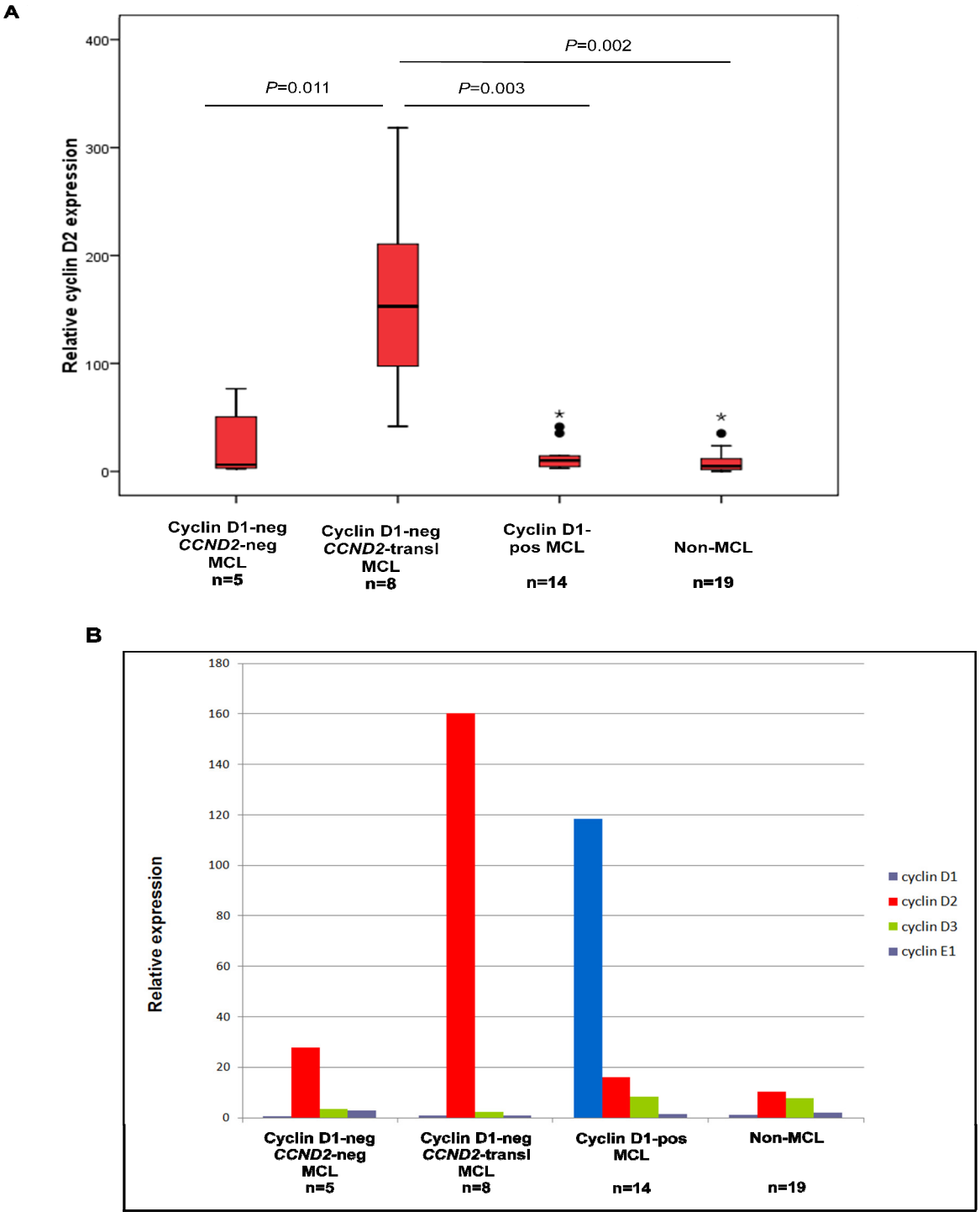

Supplemental Figure S2. Frequency of genetic alterations in *CCND2*-translocated MCL. (A) *IGK-CCND2* translocation MCL (n=7) and **(B)** *IGL-CCND2* translocation MCL(n=4). In the X-axis the chromosomes are represented horizontally from 1 to 22, in the Y-axis is represented the percentage of cases showing the copy number alterations. Gains are represented in the positive Y-axis and colored in blue, whereas losses are represented in the negative Y-axis in red.

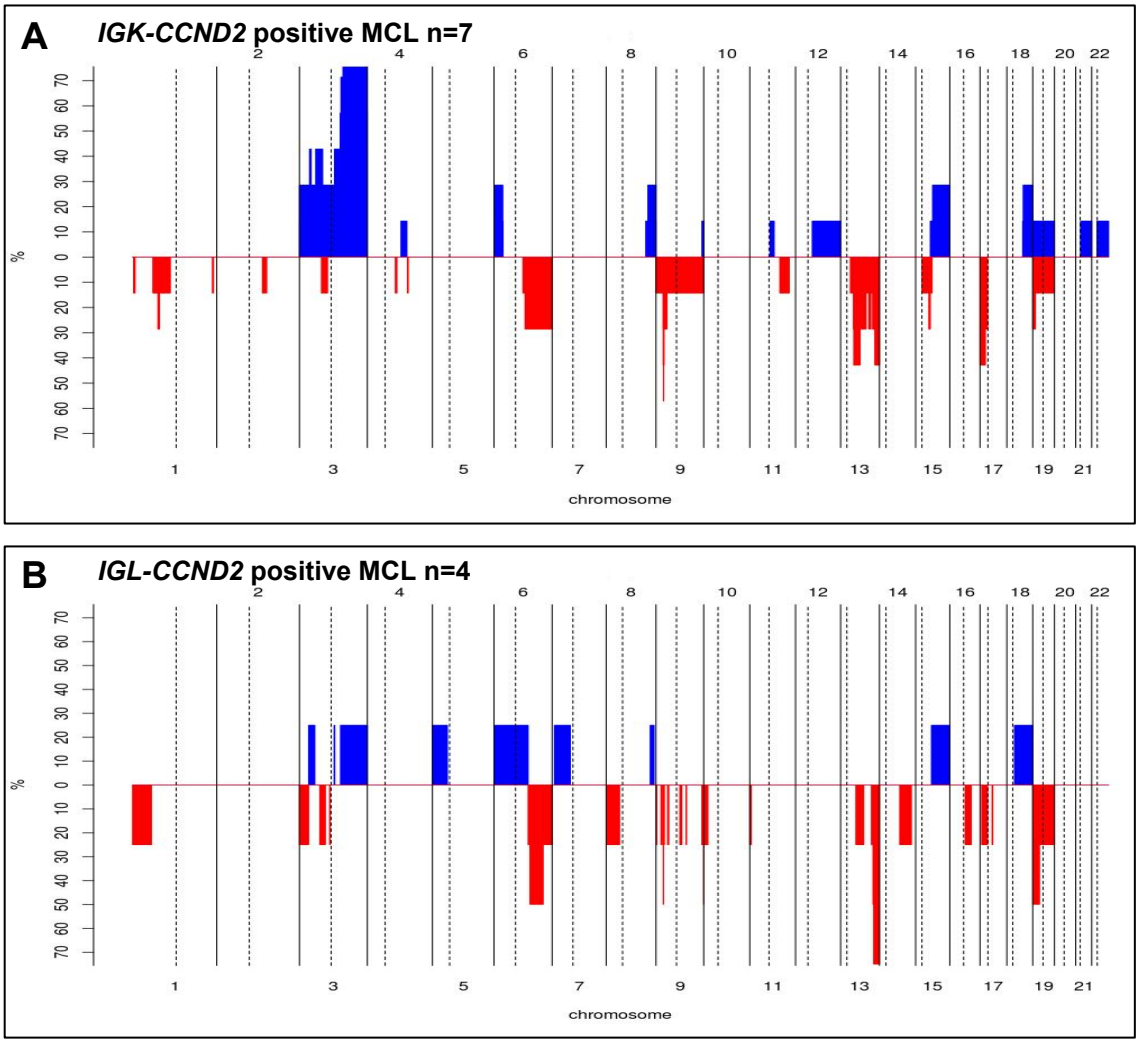

Supplemental Figure S3. Different patterns of 9p deletions in Cyclin D1-negative MCL. (A) Deletions in 9p21.3 with the minimal deleted region in *CDKN2A* gene (each black bar represents one case with deletion (n=15). **(B)** Different examples of 9p loss in four cases (deletions indicated under red rectangle). The log2 ratio for heterozygous deletions varied between -0.28 and -0.73, whereas for homozygous deletions was between -0.91 and -3.82. The heterozygous 9p deletions differed in size (2-93 Mb) and comprised a whole monosomy in two cases, whereas the homozygous 9p21 deletions diverged from a focal 68 Kb deletion (comprising the entire *CDKN2A* and part of *CDKN2B* and *MTAP* genes) to 10.3 Mb. Seven cases (47%) had deletions smaller than 2 Mb (6 homozygote and one heterozygote). All deletions spanned the *CDKN2A, CDKN2B* and *MTAP* loci. In five cases, 9p had additional deletions, besides the aforementioned 9p21.3 (range 1-4 additional losses/case).

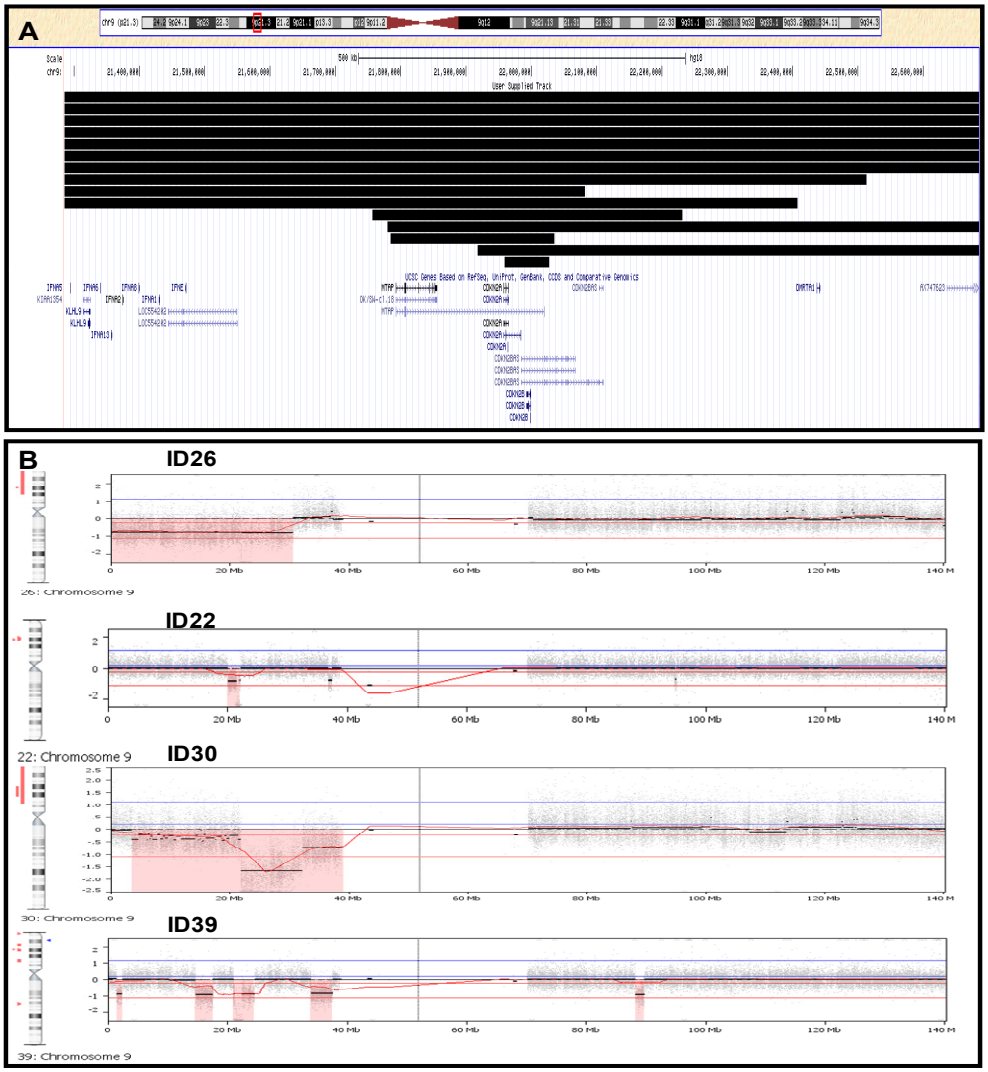

Supplemental Figure S4. Kaplan-Meier curves of Cyclin D1-negative/SOX11-positive MCL representing (A) whole series (5-year OS 48%, 95% CI, 28.4-67.6); **(B)** normal and high serum LDH levels; and **(C)** high (≥35%) and low (<35%) expression of Ki67 proliferation marker. N, number of patients; D,dead patients.

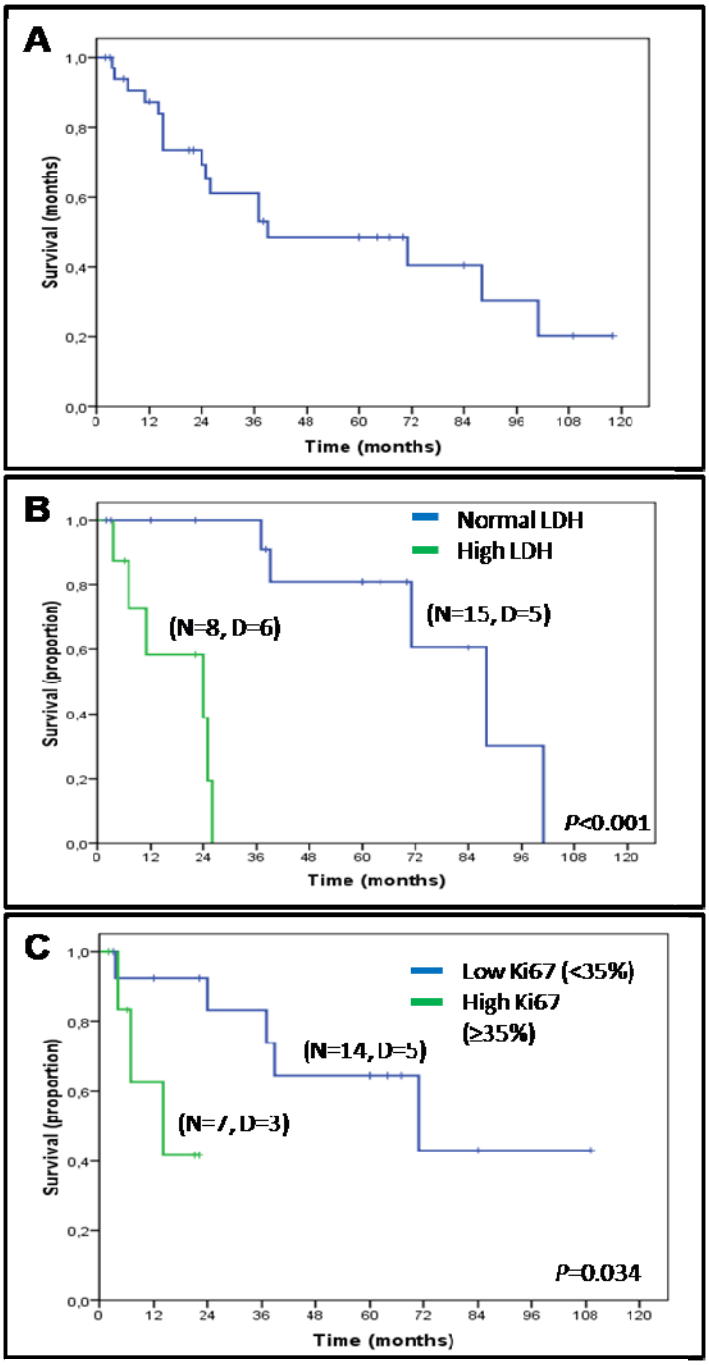

IV. Supplemental References

1. Nagel I, Szczepanowski M, Martin-Subero JI et al. Deregulation of the telomerase reverse transcriptase (TERT) gene by chromosomal translocations in B-cell malignancies. *Blood* 2010;116(8):1317-1320.

2. Zettl A, Strobel P, Wagner K et al. Recurrent genetic aberrations in thymoma and thymic carcinoma. *Am.J.Pathol.* 2000;157(1):257-266.

3. van Dongen JJ, Langerak AW, Bruggemann M et al. Design and standardization of PCR primers and protocols for detection of clonal immunoglobulin and T-cell receptor gene recombinations in suspect lymphoproliferations: report of the BIOMED-2 Concerted Action BMH4-CT98-3936. *Leukemia* 2003;17(12):2257-2317.

4. Lepretre F, Villenet C, Quief S et al. Waved aCGH: to smooth or not to smooth. *Nucleic Acids Res.* 2010;38(7):e94.

5. Royo C, Navarro A, Clot G et al. Non-nodal type of mantle cell lymphoma is a specific biological and clinical subgroup of the disease. *Leukemia* 2012; 26(8):1895-1898.